RSC Advances

ROYAL SOCIETY OF CHEMISTRY

www.rsc.org/advances

Fabrication of a Core-Shell-Shell Particle with a Quarter-Wave Thick Shells and Its optical properties

Hiroki Shibata, Kenji Imakita[*]*, and Minoru Fujii*

Department of Electrical and Electronic Engineering, Graduate School of Engineering, Kobe University, Rokkodai, Nada, Kobe 657-8501, Japan

KEYWORDS nanoparticle, multi-shelled particles, optical properties

ABSTRACT:

A multi-shelled sphere with a quarter-wave thick shells is known to act as a spherical Bragg resonator with a complete photonic band gap and have potential applications in photonics. However, no fabrication techniques have been established. In this work, core-shell-shell particles with a quarter-wave thick shells were synthesized by chemical solution processes for the first time. It consists of a Ce^{3+} doped Y_2O_3 nano particle core, a SiO_2 first shell, and a Y_2O_3 second shell. The core and the second shell were fabricated by a homogeneous precipitation method and the first shell by a sol gel method. By carefully optimizing the reaction conditions, the shell thickness was controlled to a quarter optical wavelength for visible (500 nm) light with the standard deviation of thickness of the order of several nanometers. The scattering and photoluminescence spectra of single particles were studied, and they were well reproduced by Mie theory. The results indicate that luminescent properties of nano particles can be modified by a quarter-wave thick shells. The procedures can be extended for the fabrication of multi-shelled photonic bandgap structures, by simply repeating the SiO_2 and Y_2O_3 coating processes.

A multi-shelled sphere with a quarter-wave thick shells is known to act as a spherical Bragg resonator.[1,2] When the sphere consists of a core and alternating high and low refractive index shells, the shells work as a spherical Bragg mirror and photons can be confined inside the core three-dimensionally.[3] As the core size decreases, the confinement region becomes smaller. It can reach a sub-100 nm scale, which is several orders of magnitude smaller than that in a conventional microsphere resonator utilizing whispering-gallery modes. The strong confinement significantly modifies the luminescent properties, such as radiative decay rate, of a luminescent dipole located inside the core due to the constructive or destructive interference of the near field.[4,5] For example, in case of a Y_2O_3 nano particle with the radius of 65 nm, the coating of 12 shells, consisting of TiO_2 and SiO_2, results in 500 times enhancement of the radiative decay rate at the resonant wavelength and suppression by 3 orders of magnitude at the off-resonant wavelength.[6] The size of the 12 shelled particles is about 1 micrometer. The multi-shelled particles have potential applications to phosphors with inherently low quantum efficiency, such as quantum cutting[7,8] and upconversion phosphors.[9-11]

Fabrication of a multi-shelled sphere with a quarter-wave thick shells is very challenging. Renguo Xie, et al.[12] formed multi-shells on the surface of CdSe nanocrystals by using a successive ion layer adhesion and reaction (SILAR) technique. Gia-Chi Chen, et al.[13] formed multi-shells by using reverse micelle techniques, in which nanoparticles of desired shell material are sequentially adsorbed onto the core surface through electrostatic and hydrophilic/hydrophobic interactions. In these cases, however, the shells are thinner than several nanometers. This is one order of magnitude smaller than a quarter optical wavelength for visible light and is too thin to control the radiative decay rate. In case of a single shell, much thicker shells have been reported to be formed on the surface of nanoparticles. For example, a uniform Y_2O_3 shell was synthesized by simple chemical solution processes called as a homogeneous precipitation method.[14-17] Uniform silica shells synthesized by a sol gel method have been also reported. In these reports, the shell thickness can be controlled in a wide range from nano- to submicron-scale.[18-25] However, these coating techniques were used only for the formation of a single shell. In addition, there have been no reports on the precise control of the shell thickness to obtain a quarter-wave thick shells.

In this work, we synthesize core-shell-shell particles with a quarter-wave thick shells. The particle consists of a Y_2O_3 core, a SiO_2 first shell, and a Y_2O_3 second shell. Sol-gel and

homogeneous precipitation methods were used for synthesizing SiO_2 and Y_2O_3 shells, respectively. We show that, by carefully optimizing the reaction conditions, the shell thickness can be controlled to a quarter optical wavelength for visible (500 nm) light with the standard deviation of the thickness of the order of several nanometers. The scattering and photoluminescence spectra of single particles are studied and they are well explained by Mie theory. [26-30]

Core-shell-shell particles were synthesized by chemical solution processes. Ce^{3+} doped Y_2O_3 (Y_2O_3:Ce) core was fabricated by a homogeneous precipitation method. 0.01 M yttrium nitrate ($Y(NO_3)_3$•n-H_2O, 99.99%), 0.1 mM cerium nitrate ($Ce(NO_3)_3 \cdot 6H_2O$, 98.0%) and 0.8 M urea ($(NH_3)_2CO$, 99.0%) were dissolved in distilled water and the solution was heated at 75 °C for 6 hours under vigorous stirring. The formed precipitates were then dried and annealed at 850 °C in 2 hours to form Y_2O_3:Ce particles. Figure 1a shows a TEM image of Y_2O_3:Ce core particles. The particles are well dispersed and no agglomerates are seen. The inset is the higher magnification image. The particles are almost spherical. The radius of the Y_2O_3:Ce particles can be controlled from several tens to several hundreds nanometers by urea concentration (Figure S1). In this work, the average radius is controlled to 210 nm, corresponding to third quarter optical wavelength of 500 nm for the Y_2O_3 refractive index (1.91). This size allows constructive interference of the dipole near field and leads to significant enhancement of the radiative decay rate if a quarter-wave thick shells are formed. [6] The first SiO_2 shell was prepared by a Stöber method. 3 ml NH_3 (aq, 28%), 200 μl tetraethyl orthosilicate (TEOS) and 5 ml distilled water were added to 50 ml ethanol solution containing Y_2O_3:Ce core particles. After 5 hours stirring at room temperature, a SiO_2 amorphous shell was formed. Figure 1b shows the TEM image of SiO_2 coated Y_2O_3:Ce (Y_2O_3@SiO_2) particles. The particles are spherical. In the inset, we can clearly see a SiO_2 shell on the surface of a Y_2O_3 core particle. The shell thickness is about 90 nm. This corresponds to a quarter wavelengths of 500 mm for the SiO_2 refractive index (1.45). SiO_2 shell thickness can be controlled by the concentration of the precursor (TEOS) and the catalyst (NH_3-aq) (Figure S2).[21,23,24] The second shell of Y_2O_3 is synthesized by a homogeneous precipitation method. 0.01 M yttrium nitrate and 0.8 M urea were added to distilled water containing the SiO_2 coated Y_2O_3:Ce (SiO_2@Y_2O_3) particles. The particles were then annealed at 950 °C to form a Y_2O_3 shell. Figure 1c shows the TEM image of the Y_2O_3 coated Y_2O_3@SiO_2 (Y_2O_3@SiO_2@Y_2O_3) particles. Most of the particles are spherical. The SiO_2 and Y_2O_3 shells cannot be seen because

the particles are too large for the electron beam to pass through. Figure 1d shows the size distribution of Y_2O_3:Ce, Y_2O_3@SiO_2, and Y_2O_3@SiO_2@Y_2O_3 particles, respectively. By coating the SiO_2 and Y_2O_3 shells, the distribution shifts to larger sizes. The average radius of the Y_2O_3:Ce, Y_2O_3@SiO_2, and Y_2O_3@SiO_2@Y_2O_3 is 213.8, 304.3, and 370.6 nm, respectively. The difference in the size corresponds to the shell thickness. The thickness of the SiO_2 and Y_2O_3 shells are 91 and 65 nm, respectively. The SiO_2 shell thickness is consistent with the TEM image in Figure 1b. The Y_2O_3 shell thickness is controlled to 65 nm, corresponding to a quarter optical wavelengths of 500 nm for the Y_2O_3 refractive index (1.91). It should be noted here that the size distribution does not increase by the coatings. The standard deviation (σ) of the size distribution is 17.1 nm 17.3 nm, and 18.4 nm for the Y_2O_3:Ce, Y_2O_3@SiO_2, and Y_2O_3@SiO_2@Y_2O_3 particles, respectively. This means that the shell thickness distribution is very small and the standard deviation is of the order of several nanometers. This is small enough to control the radiative decay rate by a quarter-wave thick shells.[6]

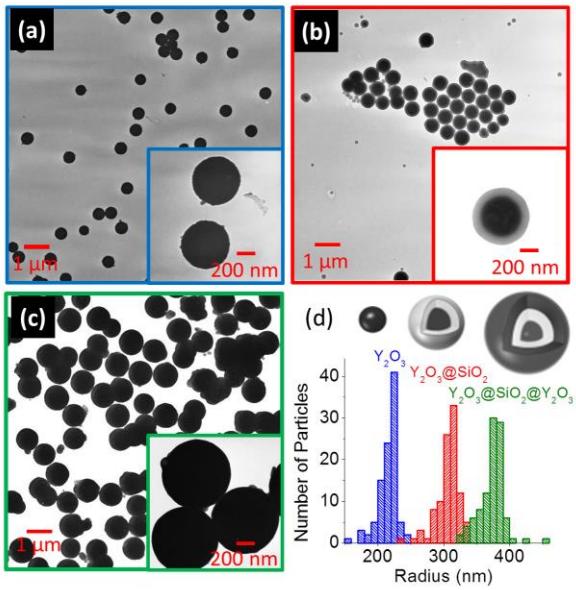

Figure 1. TEM images of the prepared (a)Y_2O_3, (b)Y_2O_3@SiO_2 and (c)Y_2O_3@SiO_2@Y_2O_3 particles. (d) The particle size distributions.

It should be noted here that the reaction temperature (65 ^oC) and the urea concentration (0.2 M) for the Y_2O_3 shell coating process are lower than those for the Y_2O_3 core formation process (75^oC, 0.8 M). In the milder reaction condition, heterogeneous nucleation on the surface of the

Y_2O_3@SiO_2 particles dominates the homogeneous nucleation, resulting in the shell formation. Y_2O_3 shell thickness can be controlled from 30 to 70 nm by varying the amount of urea from 0.10 to 0.30 M (Figure S3). This is much thicker than the report by G.Liu, et al., in which a 20 nm thick Y_2O_3 shell was formed on the surface of SiO_2 particles by using a similar method. [31]

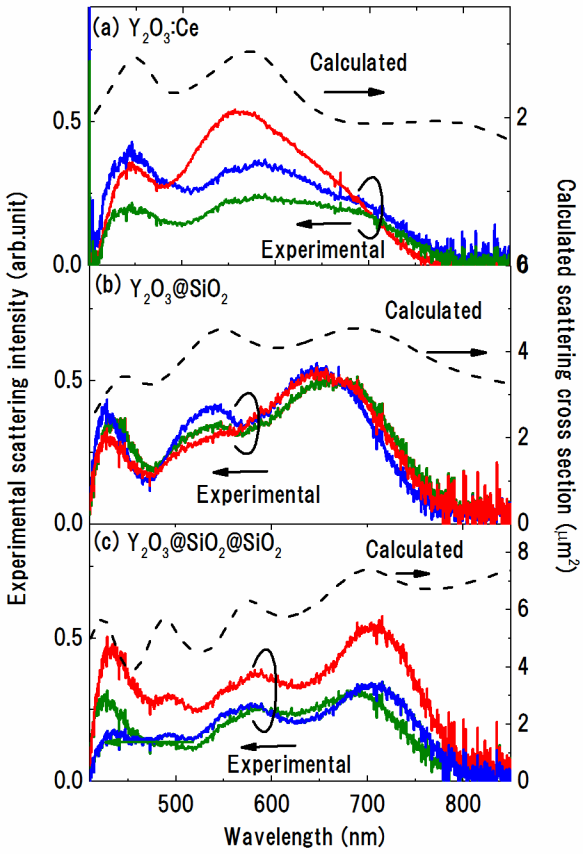

Figure 2. Experimental and calculated scattering spectra of a single particle for the (a)Y_2O_3, (b)Y_2O_3@SiO_2 and (c)Y_2O_3@SiO_2@Y_2O_3 samples. Different colors are used for different particles.

To evaluate the quality of the multi-shelled sphere, we measured the scattering and photoluminescence (PL) spectra of single particles. Figure 2a-c show some typical scattering spectra of Y_2O_3:Ce core particles, Y_2O_3@SiO_2 particles, and Y_2O_3@SiO_2@Y_2O_3 particles, respectively. The solid lines are the measured scattering spectra for 3 different particles and the dashed lines are scattering cross section spectra calculated by Mie theory.[29] Different colors are

used for different particles. The particle sizes for the calculation were obtained from Figure 1d. Several Mie resonance peaks can be seen both in the calculated and experimental results, and the number of peaks increases as the number of shells increases. The peak wavelength of the measured scattering spectra agrees well with those of calculations, although the amplitudes are not fully reproduced. Qualitatively similar results were observed for other particles (Figure S4).

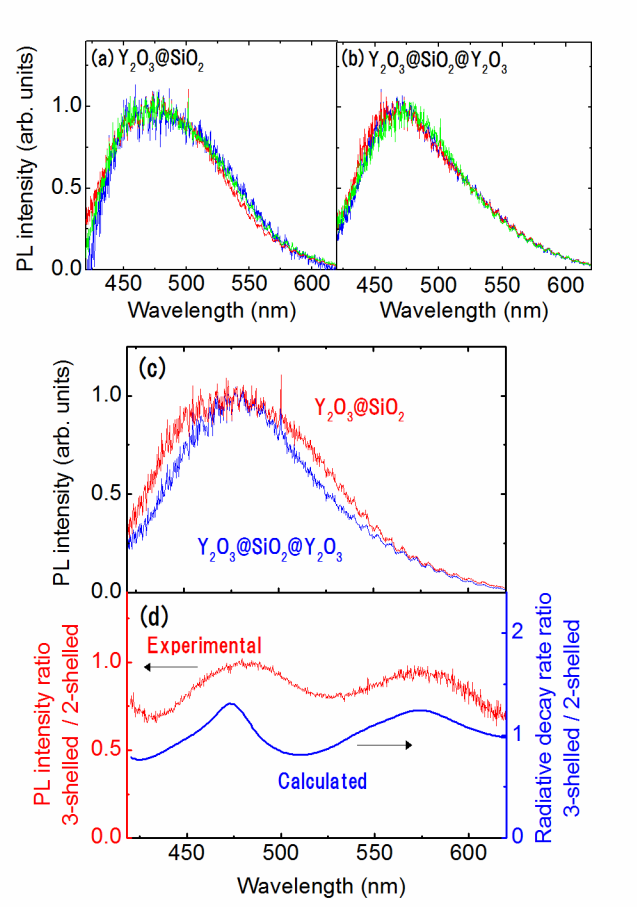

Figure 3. Normalized PL spectra of a single particle for the (a)Y_2O_3@SiO_2 and (b)Y_2O_3@SiO_2@Y_2O_3 samples. Different colors are used for different particles. (c)Comparison of the normalized PL spectra of the Y_2O_3@SiO_2 and Y_2O_3@SiO_2@Y_2O_3 samples. (d) Ratio of the normalized PL intensity of the Y_2O_3@SiO_2@Y_2O_3 particle to that of the Y_2O_3@SiO_2 one (left axis) and the calculated ratio of the radiative decay rate of a luminescent dipole inside the core of the Y_2O_3@SiO_2@Y_2O_3 particle to that of the Y_2O_3@SiO_2 one (right axis).

Ce^{3+} doped Y_2O_3 nano particles are known to show a broad PL spectrum in the visible region.[32] The broad spectrum is suitable to study the modification of radiative decay rate by the double shell. Figure 3a shows some typical PL spectra of single particles of the Y_2O_3@SiO_2 sample. Different colors are used for different particles. The spectra are normalized to the peak intensity, because the intensity varies depending on the individual particles. The raw data are shown in Figure S5. The spectral shape is almost identical for all the particles, indicating that the local environment of Ce^{3+} is similar among these particles. Similarly, single Y_2O_3@SiO_2@Y_2O_3 particles show a broad PL spectrum, whose shape does not depend on the individual particles (Figure 3b). From figure 3a and 3b, we can notice that the spectral shape of the Y_2O_3@SiO_2@Y_2O_3 particles is slightly different from that of the Y_2O_3@SiO_2 particles. Figure 3c compares the spectral shape of single Y_2O_3@SiO_2 and Y_2O_3@SiO_2@Y_2O_3 particles. The particles were randomly chosen. We can see that the PL spectrum of a Y_2O_3@SiO_2 particle becomes shaper after the Y_2O_3 shell coating. This sharpening was observed for other randomly chosen particles (Figure S6). The results imply that the Y_2O_3 shell coating modifies the PL property. Note that the local environment of Ce^{3+} is likely to be unchanged by the Y_2O_3 shell coating, because Ce^{3+} is placed inside the core surrounded by the SiO_2 shell. To discuss the modification more quantitatively, the ratios of the PL intensity of the Y_2O_3@SiO_2@Y_2O_3 particle to that of the Y_2O_3@SiO_2 one are shown in Figure 3d. The spectrum has two broad peaks around 480 and 580 nm. This can be explained by modification of radiative decay rate by the Y_2O_3 shell. The right axis shows the calculated radiative decay rate ratio of a luminescent dipole inside the core of Y_2O_3@SiO_2 to that of Y_2O_3@SiO_2@Y_2O_3. (The calculation procedures are shown in Supporting Information). We can see that the calculated ratio well reproduces the PL intensity ratio. The core radius and the thickness of the first and second shells are assumed to be 210, 91, and 65 nm, respectively, for the calculation. These are well consistent with the results of the TEM observations in Figure 1. Similar results were observed for other randomly chosen particles (Figure S7). Note that the radiative decay rate ratio is identical to the quantum efficiency ratio when the quantum efficiency is very small (See Supporting Information), and this is the case with the PL from Ce^{3+} doped in Y_2O_3 matrix.[33] These results indicate that the core-shell-shell particles with a quarter-wave shell thickness were fabricated with high accuracy.

In conclusion, we have synthesized core-shell-shell particles with a quarter-wave thick shells for the first time. It consists of the core of Ce^{3+} doped Y_2O_3 nano particle, the first shell of SiO_2,

and the second shell of Y_2O_3. The core and the second shell were fabricated by a homogeneous precipitation method and the first shell by a sol gel method. The size of the particles is uniform and the standard deviation of the shell thickness distribution is of the order of several nanometers. The scattering and photoluminescence spectra of a single particle were modified by the shell coatings and the modification was well reproduced by calculations based on Mie theory. The results indicate that the core-shell-shell structure was fabricated with high accuracy. The SiO_2 and Y_2O_3 coating processes can be alternately repeated to increase the number of shells, which could be a possible approach for fabricating the multi-shelled sphere as a spherical Bragg resonator.

SUPPORTING INFORMATION

Measurement details of PL and scattering spectra of single particles; calculation procedures of normalized radiative decay rate and the relationship with quantum efficiency; TEM images of single Y_2O_3:Ce, Y_2O_3@SiO_2, and Y_2O_3@SiO_2@Y_2O_3 particles; PL and scattering spectra of single Y_2O_3:Ce, Y_2O_3@SiO_2, and Y_2O_3@SiO_2@Y_2O_3 particles.

ACKNOWLEDGHMENT

This work was supported by KAKENHI (25790015)

AUTHOR INFORMATION

Corresponding Author

*imakita@eedept.kobe-u.ac.jp

REFERENCES

(1) M. E. Tobar, J.-M. Le Floch, D. Cros, J. Krupka, J. D. Anstie and J. G. Hartnett, Spherical Bragg Reflector Resonators. *IEEE Trans. Ultrason. Ferroelectr. Freq. Control* **2004**, *51*, 1054–1059.

(2) D. Brady, G. Papen and J. E. Sipe, Spherical Distributed Dielectric Resonators. *J. Opt. Soc. Am. B* **1993**, *10*, 644.

(3) K. Sullivan and D. Hall, Radiation in Spherically Symmetric Structures. II. Enhancement and Inhibition of Dipole Radiation in a Spherical Bragg Cavity. *Phys. Rev. A* **1994**, *50*, 2708–2718.

(4) G. Burlak, Optical Radiation from Coated Microsphere with Active Core. *Phys. Lett. A* **2002**, *299*, 94–101.

(5) A. Moroz, A Recursive Transfer-Matrix Solution for a Dipole Radiating inside and Outside a Stratified Sphere. *Ann. Phys. (N. Y).* **2005**, *315*, 352–418.

(6) K. Imakita, H. Shibata, M. Fujii and S. Hayashi, Numerical Analysis on the Feasibility of a Multi-Layered Dielectric Sphere as a Three-Dimensional Photonic Crystal. *Opt. Express*, **2013**, *21*, 11223–11230.

(7) R. T. Wégh, H. Donker, K. D. Oskam and A. Meijerink, Visible Quantum Cutting in $LiGdF_4:Eu^{3+}$ Through Downconversion. *Science* **1999**, *283*, 663–666

(8) D. Chen, Y. Yu, Y. Wang, P. Huang and F. Weng, Cooperative Energy Transfer Up-Conversion and Quantum Cutting Down-Conversion in $Yb^{3+}:TbF_3$ Nanocrystals Embedded Glass Ceramics. *J. Phys. Chem. C* **2009**, *113*, 5406–6410

(9) J. Liao, Z. Yang, H. Wu, D. Yan, J. Qiu, Z. Song Y. Yang D. Zhoua, Z. J. Yin, Enhancement of the up-conversion luminescence of Yb^{3+}/Er^{3+} or Yb^{3+}/Tm^{3+} co-doped $NaYF_4$ nanoparticles by photonic crystals. *J. Mater. Chem. C, **2013**,1, 6541-6546*

(10) P. Ghosh, J. Oliva,; E. De la Rosa, K. K. Haldar, D. Solis and A. Patra, Enhancement of Upconversion Emission of $LaPO_4$:Er@Yb Core-Shell Nanoparticles/Nanorods. *J. Phys. Chem. C* **2008**, *112*, 9650–9658

(11) F. Wang, R. Deng, F. Wang, Q. Wang, Y. Han, H. Zhu, X. Chen, X. Liu, Tuning Upconversion Through Energy Migration in Core-Shell Nanoparticles. Nature Materials, 2**011**, *10*, 967–973.

(12) R. Xie, U.Kolb, J. Li, T. Basché and A. Mews, Synthesis and Characterization of Highly Luminescent CdSe-Core $CdS/Zn_{0.5}Cd_{0.5}S/ZnS$ Multishell Nanocrystals. *J. Am. Chem. Soc.* **2005**, *127*, 7480–7488.

(13) G.-C. Chen, C.-Y. Kuo and S.-Y. Lu, A General Process for Preparation of Core-Shell Particles of Complete and Smooth Shells. *J. Am. Ceram. Soc.* **2005**, *88*, 277–283.

(14) Y. Huang, D. Jiang, J. Zhang, Q. Lin and Z. Huang, Synthesis of Mono-Dispersed Spherical Nd:Y_2O_3 Powder for Transparent Ceramics. *Ceram. Int.* **2011**, *37*, 3523–3529.

(15) J.-G. Li, X.Li, X. Sun and T. Ishigaki, Monodispersed Colloidal Spheres for Uniform $Y_2O_3:Eu^{3+}$ Red-Phosphor Particles and Greatly Enhanced Luminescence by Simultaneous Gd^{3+} Doping. *J. Phys. Chem. C* **2008**, *112*, 11707–11716.

(16) B. Tissue and H. Yuan, Structure, Particle Size, and Annealing of Gas Phase-Condensed $Eu^{3+}:Y_2O_3$ Nanophosphors. *J. Solid State Chem.* **2003**, *171*, 12–18.

(17) H. Wang; C. K. Lin, X. M. Liu, J. Lin and M. Yu, Monodisperse Spherical Core-Shell-Structured Phosphors Obtained by Functionalization of Silica Spheres with Y_2O_3:Eu^{3+} Layers for Field Emission Displays. *Appl. Phys. Lett.* **2005**, *87*, 181907.

(18) S. H. Joo, J. Y. Park, C.-K. Tsung, Y. Yamada, P. Yang and G. A. Somorjai, Thermally Stable Pt/mesoporous Silica Core-Shell Nanocatalysts for High-Temperature Reactions. *Nat. Mater.* **2009**, *8*, 126–131.

(19) J. Kim, H. S. Kim, N. Lee, T. Kim, H. Kim, T. Yu, I. C. Song, W. K. Moon and T. Hyeon, Multifunctional Uniform Nanoparticles Composed of a Magnetite Nanocrystal Core and a Mesoporous Silica Shell for Magnetic Resonance and Fluorescence Imaging and for Drug Delivery. *Angew. Chem. Int. Ed. Engl.* **2008**, *47*, 8438–8441.

(20) Y. Kobayashi, M. Horie, M. Konno, B. Rodríguez-González,; L. M. Liz-Marzán, Preparation and Properties of Silica-Coated Cobalt Nanoparticles †. *J. Phys. Chem. B* **2003**, *107*, 7420–7425.

(21) H. B. Lee, Y. M. Yoo and Y.-H. Han, Characteristic Optical Properties and Synthesis of Gold–silica Core–shell Colloids. *Scr. Mater.* **2006**, *55*, 1127–1129.

(22) T. Liu, W. Xu, X. Bai and H. Song, Tunable Silica Shell and Its Modification on Photoluminescent Properties of Y_2O_3:Eu^{3+}@SiO_2 Nanocomposites. *J. Appl. Phys.* **2012**, *111*, 064312.

(23) L. M. Liz-Marzán, M. Giersig, P. Mulvaney, Synthesis of Nanosized Gold−Silica Core−Shell Particles. *Langmuir* **1996**, *12*, 4329–4335.

(24) E. Mine, A. Yamada, Y. Kobayashi, M. Konno, L. M. Liz-Marzán, Direct Coating of Gold Nanoparticles with Silica by a Seeded Polymerization Technique. *J. Colloid Interface Sci.* **2003**, *264*, 385–390.

(25) Q. Zhang, J. Ge, J. Goebl, Y. Hu, Z. Lu, Y. Yin, Rattle-Type Silica Colloidal Particles Prepared by a Surface-Protected Etching Process. *Nano Res.* **2010**, *2*, 583–591.

(26) C. F. Bohren, D. R. Huffman. *Absorption and Scattering of Light by Small Particles*, Wiley-VCH Verlag GmbH: Weinheim, Germany, 1998, p. 530.

(27) Z. S. Wu and Y. P. Wang, Electromagnetic Scattering for Multilayered Sphere: Recursive Algorithms. *Radio Sci.* **1991**, *26*, 1393–1401.

(28) J. Sinzig, Quinten, M. Scattering and Absorption by Spherical Multilayer Particles. *Appl. Phys. A Solids Surfaces* **1994**, *58*, 157–162.

(29) B. R. Johnson, Light Scattering by a Multilayer Sphere. *Appl. Opt.* **1996**, *35*, 3286–3296.

(30) M. I. Mishchenko, Light Scattering by Randomly Oriented Axially Symmetric Particles. *J. Opt. Soc. Am. A* **1991**, *8*, 871.

(31) G. Liu and G. Hong, Synthesis of SiO_2/Y_2O_3:Eu Core-Shell Materials and Hollow Spheres. *J. Solid State Chem.* **2005**, *178*, 1647–1651.

(32) M. Raukas, A. Konrad, and K. C. Mishra, Luminescence in nano-size Y_2O_3:Ce. J. Luminescence, **2007**, *122-123*, 773-775.

(33) M. Raukas, S. A. Basun, W. V. Schaik, W. M. Yen and U. Happek, Luminescence efficiency of cerium doped insulators: The role of electron transfer processes. Appl. Phys. Lett., *1996*, *69*, 3300–3302.